[1] Fracxicon as a hybrid element between the parabolic lens and the linear axicon

Ustinov A.V., Khonina S.N.
Image Processing Systems Institute, Russian Academy of Sciences
Samara State Aerospace University

Abstract

In previous studies we have shown on the basis of the geometrical-optical analysis that the fracxicon (generalized optical element of the parabolic lens and the linear axicon) formally produces an infinitely large value of the intensity on the optical axis. Within the framework of the paraxial wave model this caustic effect was not found. In this paper, we consider plane wave diffraction on the fracxicon in nonparaxial wave model and we show that at high numerical aperture the fracxicon with an exponent close to 3/2, is actually an analogue of the hyperbolic lens optimally focusing incident beam.

Keywords: *fracxicon, parabolic lens, axicon, hyperbolic lens, high numerical aperture.*

Citation: *Ustinov AV. Fracxicon as a hybrid element between the parabolic lens and the linear axicon / Ustinov A.V., Khonina S.N. // Computer Optics. – 2014. – Vol. 38(3). – P. 402-411.*

Introduction

In paper The Axicon: A New Type of Optical Element by J.H. McLeod 1954 [1] the axicon meant any optical element possessing an axial symmetry which, due to its image and/or diffraction, transfers the light from the point source located on the optical axis to an axial segment. Later on, the classical axicon gave its name to an optical element, the phase function of which has linear dependence on the radius – the linear or conic axicon [2]. At the same time different options were proposed for axially symmetrical optical elements forming an axial light section with certain properties including the logarithmic axicon [3-5], the generalized axicon [6] and the axilens [7]. Tandem of the lens and the axicon – the lensacon [8-10] also possesses some interesting properties, which allows to form conic axial distributions.

Thus, the basic difference between the axicon and the lens that shows a point source as a point is to form a long length focus. Unfortunately, this advantage of the axicon is accompanied by a low quality image of extra-axis points [11-13]. Another advantage of the axicon, i.e. the image of the point with a smaller transverse dimension than that provided by the lens with the same numerical aperture, has also a disadvantage since it is accompanied by a higher level of side lobes that prevent to obtain a quality image.

Therefore, usually, the axicon is efficiently used in other applications: in metrology [14, 15], in nondestructive testing of materials and devices [16, 17], in scanning biometric systems [18-22], in optical micromanipulation [23-26].

In paper [27] a new diffractive optical element was proposed, the phase function of which is represented in the form of exponential function of the radius. Since the exponent γ was supposed to be any positive real number, including a fractional number, the element was named the fracxicon. The conical axicon and the parabolic lens are particular cases of the fracxicon.

Depending on its parameters, the fracxicon can act similarly to the lensacon, i.e. it can form a longitudinal light segment of a conical form (with a scale-changing dimension) or to the logarithmic axicon. In general cases, the fracxicon is a new optical element and increases opportunities of the known elements mentioned in the above applications.

In paper [28], based on the geometrical-optical analysis, it was shown that the fracxicon with the exponent $1<\gamma<2$ formally allows to produce an infinitely large value of the intensity on the optical axis. Within the framework of the paraxial wave model this caustic effect was not found [29]. In this paper we consider the effect of the fracxicon as a transition element between the parabolic lens ($\gamma=2$) and the axicon ($\gamma=1$) in a nonparaxial wave model.

1. Axial distribution while illuminating the fracxicon by the plane wave in a nonparaxial wave model for $1 < \gamma < 2$

Let us consider a field on the optical axis under conditions of the radial symmetry:

$$E(0,0,z) = \\ = -\frac{z}{2\pi}\int_0^R E_0(r)\frac{\exp\left(ik\sqrt{r^2+z^2}\right)}{\left(r^2+z^2\right)}\left(ik-\frac{1}{\sqrt{r^2+z^2}}\right)r\,\mathrm{d}r, \quad (1)$$

where $E_o(r)$ – is an input field limited with a pupil with the radius R, $k=2\pi/\lambda$ – is a wave number, and λ – is the wave length.

In paper [30] it was shown that for the correct analysis the formula (1) can be conveniently represented in the following form:

$$E(0,0,z) = \\ = E_0(0)\exp(ikz) - E_0(R)\frac{z\cdot\exp\left(ik\sqrt{R^2+z^2}\right)}{\sqrt{R^2+z^2}} + \\ +z\cdot\int_0^R\frac{\mathrm{d}E_0(0)}{\mathrm{d}r}\frac{\exp\left(ik\sqrt{r^2+z^2}\right)}{\sqrt{r^2+z^2}}\mathrm{d}r. \quad (2)$$

In case of diffraction of the plane wave on the fracxicon [27, 29] in the approximation of a thin element the input field has the following view:

$$E_0(r) = \exp(-i\alpha r^\gamma) \quad (3)$$

where $\alpha = (k\alpha_o)^\gamma$, α_o – is a dimensionless coefficient related to the numeric aperture of the optical element and defining the focusing degree.

Then, the formula (2) would be written down in the following way:

$$E(0,0,z) = E_\gamma(z) - \\ -i\gamma\left(k\alpha_0\right)^\gamma z\cdot\int_0^R\frac{\exp\left(ik\sqrt{r^2+z^2}-i\left(k\alpha_0 r\right)^\gamma\right)}{\sqrt{r^2+z^2}}r^{\gamma-1}\,\mathrm{d}r, \quad (4)$$

where

$$E_\gamma(z) = \exp(ikz) - \\ -\exp\left(-i\left(k\alpha_0 R\right)^\gamma\right)\frac{z\cdot\exp\left(ik\sqrt{R^2+z^2}\right)}{\sqrt{R^2+z^2}}.$$

We can approximately calculate the formula (4) using the modified method of a stationary phase [29]:

$$E(0,0,z) \approx E_\gamma(z) - iz\gamma\left(k\alpha_0\right)^\gamma A(r_0)\times \\ \times\exp\left[ik\psi(r_0)\right]\sqrt{\frac{2}{\left|\psi''(r_0)\right|}}\int_{t_1}^{t_2}\exp\left(it^2\right)\mathrm{d}t, \quad (5)$$

where

$$t_1 = -r_0\sqrt{\left|\psi''(r_0)\right|/2}$$

$$t_2 = \left(R-r_0\right)\sqrt{\left|\psi''(r_0)\right|/2}$$

$$A(r_0) = \frac{kr_0}{\gamma\left(k\alpha_0\right)^\gamma\left(r_0^2+z^2\right)} \quad (6)$$

$$\psi(r_0) = k\sqrt{r_0^2+z^2} - \left(k\alpha_0 r_0\right)^\gamma \quad (7)$$

$$\psi''(r_0) = -\frac{k}{\sqrt{r_0^2+z^2}}\left((1-\gamma)+\frac{z^2}{r_0^2+z^2}\right) \quad (8)$$

here r_o – is a stationary point which is determined from the following equation:

$$\left(k\alpha_0\right)^\gamma\gamma r_0^{\gamma-1} = \frac{kr_0}{\sqrt{r_0^2+z^2}} \quad (9)$$

In the general case, the equation (9) can not be solved analytically, therefore the specific values γ should be considered for the theoretical analysis. In paper [30] such analysis was carried out for $0 < \gamma <= 1$. The range $1 < \gamma < 2$ is considered hereby below.

1.1. Distribution in the illuminated portion of the optical axis

We can deduce from the formula (9) an implicit dependence function of the stationary point to the distance. Function $z(r_o)$ has the following form:

$$z^2 = \frac{k^{2-2\gamma}}{\gamma^2\alpha_0^{2\gamma}}r_0^{4-2\gamma} - r_0^2 \quad (10)$$

Given that $0 < 4 - 2\gamma < 2$, the degree of the first summand is less than that one of the second summand, so the situation will be significantly different from $0 < \gamma < 1$ [30]. The type of the function (10) for different value ranges of the parameter γ is shown in Fig. 1.

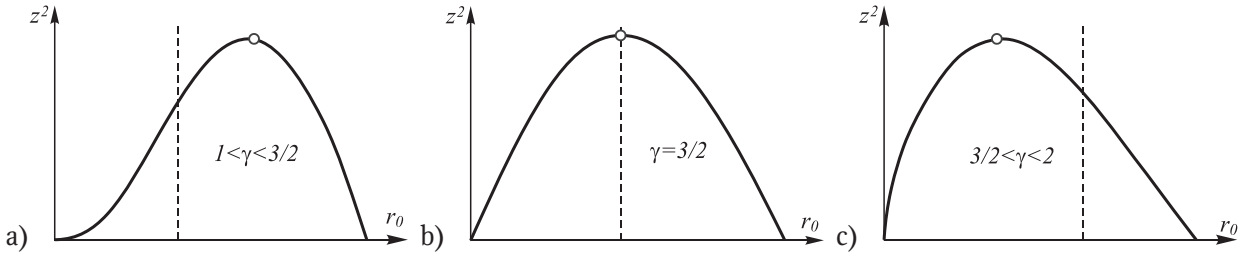

Fig. 1. Dependence function of the stationary point r_0 and the distance z

For the given value of z we may have 0, 1 or 2 stationary points. The highest value of *z*, for which there is a stationary point, equals to the following:

$$z_{\max}^2 = \frac{1}{k^2}\cdot\left(\frac{2-\gamma}{\gamma^2\alpha_0^{2\gamma}}\right)^{1/(\gamma-1)}\cdot\frac{\gamma-1}{2-\gamma} \qquad (11)$$

This is the right shadow boundary, and its nature is different from the similar boundary for the range $0 < \gamma < 1$. The shadow turned out there just because of the availability of a confining pupil (the formula for the shadow line included also its radius). Here the shadow will appear as desired for a fairly large pupil, and its appearance corresponds to the boundary of full internal reflection in the geometric-optical consideration [28].

At the same time z_{max} is the distance when, if approaching it *leftward*, two stationary points run into one another that is plotted in Fig. 2 as almost a horizontal interval. In the *formal* application of the classical method of the stationary phase we obtain an infinite amplitude to the left on the *shadow* boundary (since $f''(r_o)=0$), and a zero – to the right. The modified method of the stationary phase will formally also give an infinite value. Here below, correct values will be calculated based on more precise analysis.

This effect is similar to the infinite intensity if considering the geometric-optical analysis of the generalized lens within the same range γ [28]. Note that within the framework of the paraxial approximation this effect is not expected and not observed [29]. Let us call a point located at a distance (11) from the element as the focus point. Here is the relevant value of the stationary point.

$$r_{0,\max} = \frac{1}{k}\left(\frac{2-\gamma}{\gamma^2\alpha_0^{2\gamma}}\right)^{1/(2\gamma-2)} = z_{\max}\sqrt{\frac{2-\gamma}{\gamma-1}} \qquad (12)$$

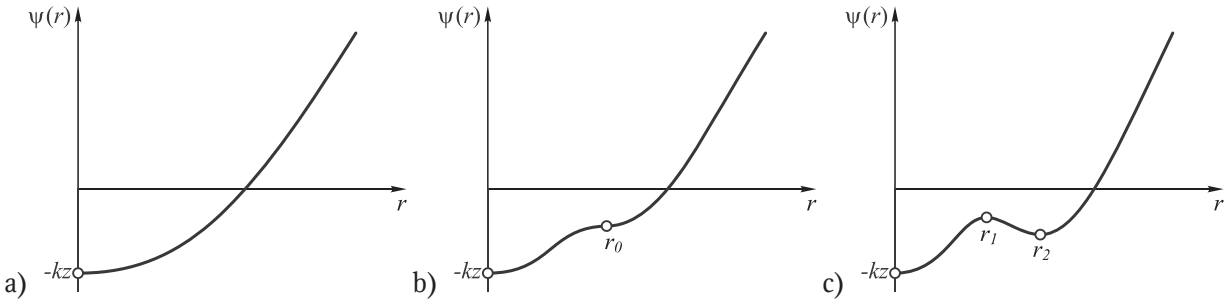

Fig. 2. View of the phase function with a different number of stationary points

The radical expression in (12) is less than 1, when $\gamma > 3/2$, and, if otherwise, is more than or equal to 1. To observe the focus, this point must get inside the pupil: $R > r_{o,max}$, i.e. the angle, at which the pupil is seen at the focus, will satisfy the following inequation:

$$\operatorname{tg}\beta = (R/z_{\max}) > (r_{0,\max}/z_{\max}) = \sqrt{(2-\gamma)/(\gamma-1)}$$

In particular, when γ = 3/2, the angle should be greater than 45°.

Let us return to the question of the amplitude value in the focus. In fact, there is no infinity existed; it is necessary to consider only the following normally rejected summand of the Taylor series for the phase (7):

$$\psi(r) \approx \psi(r_0) + \psi'''(r_0)(r-r_0)^3/6 \qquad (13)$$

To understand the properties of the fracxicon within this range we shall consider a specific value γ = 3/2 (a general case will be considered later), for which the equation (10) is algebraically solvable with respect to r_o. If substituting γ = 3/2 in (10), the following equation will be obtained:

$$z^2 = \frac{4r_0}{9k\alpha_0^3} - r_0^2 \qquad (14)$$

In this case, the curve in Fig. 1 will be symmetric with respect to the vertex (parabola). The equation has the following solution:

$$r_0 = \frac{2}{9k\alpha_0^3} \pm \sqrt{\frac{4}{81k^2\alpha_0^6} - z^2} \qquad (15)$$

The focus is located in the point $z_m = 2/9\ ka^3{}_o$, and it corresponds to the stationary point r_{om} with the same value (it also follows from the equation (12)). In the future, the values for the phase function at this point shall be used:

$$\psi(r_{0,\max}) = -\frac{4\sqrt{2}}{27\alpha_0^3};$$
$$\psi'''(r_{0,\max}) = \frac{81}{8\sqrt{2}}k^3\alpha_0^6. \qquad (16)$$

Let us estimate the size of 2Δr of the "almost horizontal" segment of the phase function (Fig. 2).

Proceeding from the fact that the phase changes on it by not more than π (more precisely: $\psi(r_{o,max} \pm \Delta r) = \psi(r_{o,max}) \pm \pi/2$) and the formula (13), we will find that (the module is not written since the third derivative is positive):

$$\Delta r = \sqrt[3]{\frac{3\pi}{\psi'''\left(r_{0,\max}\right)}} \tag{17}$$

In the first approximation of the amplitude evaluation we will take the phase constant in this interval, and the remainder of the integration interval will not be taken into account:

$$\begin{aligned}
&\int_0^R A(r)e^{i\psi(r)}\mathrm{d}r \approx 2A\left(r_{0,\max}\right)e^{i\psi\left(r_{0,\max}\right)}\Delta r = \\
&= 2A\left(r_{0,\max}\right)e^{i\psi\left(r_{0,\max}\right)}\sqrt[3]{\frac{3\pi}{\psi'''\left(r_{0,\max}\right)}} \approx \\
&\approx \frac{4,22A\left(r_{0,\max}\right)e^{i\psi\left(r_{0,\max}\right)}}{\sqrt[3]{\psi'''\left(r_{0,\max}\right)}}.
\end{aligned} \tag{18}$$

More accurate solution, whereas for any $1 < \gamma < 2$, will be evaluated if proceed similarly to the classical method of the stationary phase, i.e. expanding the limits to the infinites:

$$\begin{aligned}
&\int_0^R A(r)e^{i\psi(r)}\mathrm{d}r \approx \\
&\approx A\left(r_{0,\max}\right)e^{i\psi\left(r_{0,\max}\right)}\int_0^R e^{i\psi'''\left(r_{0,\max}\right)\left(r-r_{0,\max}\right)^3/6}\mathrm{d}r \approx \\
&\approx A\left(r_{0,\max}\right)e^{i\psi\left(r_{0,\max}\right)}\int_{-\infty}^{\infty} e^{i\psi'''\left(r_{0,\max}\right)x^3/6}\mathrm{d}x = \\
&= A\left(r_{0,\max}\right)e^{i\psi\left(r_{0,\max}\right)}\sqrt[3]{\frac{6}{\psi'''\left(r_{0,\max}\right)}}\frac{2}{3}\int_0^{\infty}\frac{\cos t}{t^{2/3}}\mathrm{d}t \approx \\
&\approx \frac{2,81A\left(r_{0,\max}\right)e^{i\psi\left(r_{0,\max}\right)}}{\sqrt[3]{\psi'''\left(r_{0,\max}\right)}}.
\end{aligned} \tag{19}$$

The latest equation in (19) is deduced with regard to the equation $\int_0^{\infty} t^{-2/3}\cos t\,\mathrm{d}t = \sqrt{3}\Gamma(1/3)/2$ [31].

Thus, the result (18) is obviously an approximation to excess.

Beyond the range of the focus neighborhood, if the two stationary points r_{o1} and r_{o2} are not too close to each other, then for each point individually you can use the formula (5), taking into account that the signs of the second derivative in the stationary points are just the opposite. The limits of integration for the summands will be as follows: $[0;(r_{01}+r_{02})/2]$ and $[(r_{01}+r_{02})/2;R]$.

Let us find the proximity criterion for the stationary points. We shall assume that the stationary points are close to each other, if their low-phase change neighborhoods overlap:

$$r_{01} + \Delta r_1 > r_{02} - \Delta r_2 \tag{20}$$

Reasoning similarly to the formula derivation (17), we shall obtain that

$$\Delta r_{1,2} = \sqrt{\pi / \left|\psi''\left(r_{01,2}\right)\right|} \tag{21}$$

If roots are similar, then in order to maintain the continuity in the transition to the focus point, we shall take the weighted sum of the result of the formula (5) and the result of the formula (18) or (19). We take the weight function of the first summand equal to $(r_{02}-r_{01})/(\Delta r_1+\Delta r_2)$, and the second weight function will be a complement-on-one.

For $\gamma = 3/2$ we would obtain the most direct quantitative results. Length of a straight line in (17) is equal to $\Delta r = (2/3k\alpha_0^2)\cdot\sqrt[3]{\pi}\cdot\sqrt[6]{2}$. Then, we will have in (18) the following:

$$\int_0^R A(r)e^{i\psi(r)}\mathrm{d}r \approx \frac{4\sqrt[3]{\pi}\sqrt[6]{2}}{3k\alpha_0^2}A\left(r_{0,\max}\right)e^{i\psi\left(r_{0,\max}\right)}. \tag{22}$$

Respectively, (19) will be converted to

$$\int_0^R A(r)e^{i\psi(r)}\mathrm{d}r \approx \frac{2\Gamma(1/3)\sqrt{6}}{9k\alpha_0^2}A\left(r_{0,\max}\right)e^{i\psi\left(r_{0,\max}\right)}. \tag{23}$$

Stationary points will be considered as similar (see the condition (20)), if the following inequation is solved

$$\Delta z < \frac{\sqrt[3]{2\pi^2/9}}{k\alpha_0} \tag{24}$$

The in equation (24) is obtained assuming that $\Delta z/z_{max}$ is small, that is similar to the requirement to have the following low value $\alpha_0^2\cdot\sqrt[3]{81\pi^2/4} \approx 5,847\alpha_0^2$

Let us find out how much will be the amplitude at the focus point compared with the amplitude at the boundary of the proximity to stationary points. With no regard to integrated summands in (2) and assuming that the factors multiplying the integral are approximately equal, we can only compare the values of the integrals. The value at the focus is given by the formula (23). The value at the boundary is obviously equal to the sum of contributions of both stationary points. Using the fact that at the boundary the point $r_{o,max}$ lies *in the middle* of the stationary points, it can be proven that by assuming from the inequation (24) the multiplication factors $A(r)e^{i\psi(r)}\sqrt{2/|\psi''(r)|}$ in the resulted equation could be considered similar when using the method of the stationary phase. In this connection the multipli-

cation factors without derivatives are taken at the point $r_{o,\,max}$, and the second derivatives are taken in the stationary points themselves. They are equal in module, but opposite in sign:

$$\psi''(r_{02}) \approx -\psi''(r_{01}) \approx \frac{27k^2\alpha_0^{9/2}}{4\sqrt{2}}\sqrt{k\Delta z}$$

Let us note that the equation is approximate, since the phase function contrary to the graph (10) does not become symmetric with respect to the point $r_{o,\,max}$.

For estimation we apply the classical method of the stationary phase. Due to different signs of the second derivative, the overall contribution of two stationary points will be not two times, but only $\sqrt{2}$ times more, than that of the one point. If we consider that on the area boundary the inequation (24) becomes the equation, the value of the integral would equal to the following:

$$\int_0^R A(r)e^{i\psi(r)}dr \approx \frac{2\sqrt[3]{4\pi/3}}{3k\alpha_0^2}A\left(r_{0,\max}\right)e^{i\psi\left(r_{0,\max}\right)} \qquad (25)$$

By dividing the values of (23) and (25) we shall find that the amplitude at the focus exceeds the amplitude on the boundary of the proximity by $\Gamma(1/3)/(\sqrt[3]{\pi}\cdot\sqrt[6]{6}) \approx 1{,}357$ times. Thus, the peak of the focus is not very sharp.

For other values of γ nothing has fundamentally changed within this range, except, perhaps, the sections located in proximity of 1 or 2. The significant qualitative change, though quantitatively it may not be very large, shall be the lack of the symmetry of stationary points related to position corresponding to the focus.

1.2. Distribution in the shadow

Let us now consider the calculations in the shadow area on the right, when $z > z_{max}$. This is a more difficult task if compared with the shadow from the entrance pupil. In case of the shadow of the pupil the modified method of the stationary phase can be applied, which, in contrast to the classical one, does not require a stationary point to be located inside the interval of integration. However, the accuracy of the approximation will fall while further proceeding deep into the shadow area. In the case under consideration, no stationary point is available in the shadow, but it does exist outside the shadow area in contrast to $\gamma = 1$, $\alpha_0 \geq 1$, where it does not exist in any situation. Therefore, it is desirable to maintain the transition persistence in calculations.

The easiest way that should work in proximity to the shadow boundary is the *formal* substitution of a *non-real number* r_o in the formula (5). Nevertheless, the formula type will not change, but you can not assume that the accumulation factor $e^{i\psi(r_0)}$ is equal in absolute value to one.

If there is no need to proceed far enough to the area, the issue will be simplified: in the vicinity of the maximum the curve (10) will be brought nearer by the parabola, that would provide an explicit formula, though an approximation, similar to (15), with arbitrary γ.

It can be shown that when properly choosing the sign of the imaginary component, while extracting a root, the amplitude in the shadow area (without regard to integrated summands) shall decay exponentially to zero while increasing the distance from the shadow boundary. This is similar to the case of $\gamma = 1$, $\alpha_o > 1$ [32].

2. Axial distribution of the parabolic lens while illuminating by the plane wave

For this particular case the function *(γ = 2) z (r_o)* has the following form:

$$z^2 = \frac{1}{4k^2\alpha_0^4} - r_0^2 \qquad (26)$$

The graph for (26) is the parabola with a node on the axis $r_o = 0$ (Fig. 3).

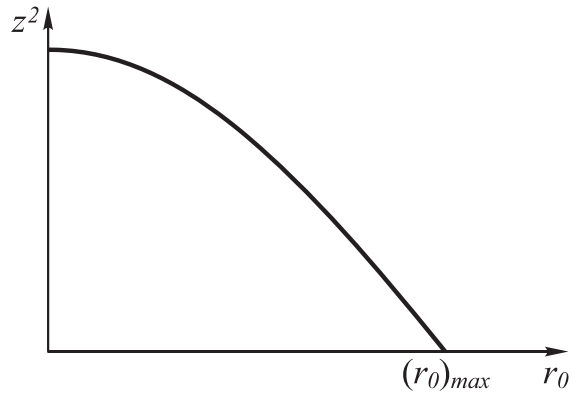

Fig. 3. Dependance function of the stationary point r_0 and the distance z, where γ = 2

For specified value of z it may be only one, or not a single, stationary point. The explicit solution is given as follows:

$$r_0 = \sqrt{\frac{1}{4k^2\alpha_0^4} - z^2} \qquad (27)$$

The maximum value equals to $r_{0,\max} = 1/2k\alpha_0^2$. If the radius *R* of the entrance pupil is smaller than this value, the shadow area will appear in prox-

imity of the optical element. Along with the range of $1 < \gamma < 2$ at any radius R there will be the shadow at the area $z > z_{\max} = 1/2k\alpha_0^2$. The shadow boundary corresponds to a multiple root; the second derivative of the phase function equals to zero, however, unlike the range of $1 < \gamma < 2$, when applying the stationary phase method, there will be no infinite amplitude, even formally. The thing is that the shadow boundary is reached at the stationary point which equals to zero, and the fraction is reduced. Let us give explicit expressions provided that at $\gamma = 2$ a slowly varying factor equals to $r/\sqrt{r^2+z^2}$:

$$\left.\begin{aligned}&\psi''(r_0) = 2k^2\alpha_0^2(1-4k^2\alpha_0^4 z^2)\\ &A(r_0) = r_0/\sqrt{r_0^2+z^2} =\\ &\quad r_0\cdot 2k\alpha_0^2 == \sqrt{1-4k^2\alpha_0^4 z^2}\end{aligned}\right\} \to \frac{A(r_0)}{\sqrt{\psi''(r_0)}} = \\ = \frac{1}{\sqrt{2}k\alpha_0} = \text{const}. \tag{28}$$

Substitution to (5) gives the following result:

$$E(0,0,z) = E_{\gamma=2}(z) - \\ -2ik\alpha_0 z\exp\left[-i\psi(r_0)\right]\int_{t_1}^{t_2}\exp\left(it^2\right)\mathrm{d}t, \tag{29}$$

where $t_1 = -r_0\sqrt{|\psi''(r_0)|/2}$

$t_2 = (R-r_0)\sqrt{|\psi''(r_0)|/2}$

Thus, when using the modified method of the stationary phase, the amplitude at the given point will not only be formally infinite, but it would be equal to zero (without regard to integrated summands) since both integration limits will equal to zero, too. By ignoring the edge summands we shall obtain the linear growth of the amplitude, if keeping in view the nodal line.

If we want to find a more accurate (non-zero) value of the amplitude in proximity of the "focus", we can argue as in the beginning of section 1.1. The difference of section 1.1 is that the third derivative at the point $r_o = 0$ also equals to zero, so we have to use the fourth derivative and represent the phase as $\psi(r) \approx \psi(r_o) + \psi^{IV}(r_o)(r\text{-}r_o)^4/24$. The dimension Δr of the "almost horizontal" segment of the phase function equals to

$$\Delta r = \sqrt[4]{\frac{12\pi}{f^{IV}(r_0)}} = \sqrt[4]{\frac{\pi}{2}}\cdot\frac{1}{k\alpha_0^{3/2}} \tag{30}$$

The slowly varying accumulation factor $r/\sqrt{r^2+z^2}$ can not be taken out from the integral sign even in the first approximation (there will be a zero), but as in 1.1, let us assume the phase in this segment as stationary, and the rest of the integration interval will not be taken into account:

$$\int_0^R \frac{r}{\sqrt{r^2+z^2}}e^{i\psi(r)}\mathrm{d}r \approx \frac{e^{i\psi(r_0)}}{z_{\max}}\cdot\int_0^{\Delta r} r\,\mathrm{d}r = \\ = e^{i\psi(r_0)}\sqrt{\pi/2}\cdot\frac{1}{k\alpha_0}. \tag{31}$$

In the last equation the explicit expressions have been substituted for z_{max} and Δr. In other words, in proximity of the shadow boundary we have

$$E(0,0,z) = E_{\gamma=2}(z) - ik\sqrt{2\pi}\alpha_0 z\exp\left[-i\psi(r_0)\right]. \tag{32}$$

The last summand in (32) happened to be not so small as we had expected; it is only by $\sqrt{2}$ times less in modulus than if we would have in (29) in the classical method of the stationary phase.

In the shadow area we can operate in the same manner as in 1.2 substituting nonreal values r_o, especially as there is an explicit formula (27). In proximity of the shadow boundary it will give a continuous transition. If proceed further deeply into the shadow area, then, starting from a certain point, in (29) the main contribution will be given by the first two integrated summands.

3. Results of numerical simulation

In numerical simulation we compared the operation of the axicon ($\gamma = 1$), the fracxicon ($\gamma = 1.5$) and the parabolic lens ($\gamma = 2$) for high values of numerical aperture. The calculation was carried out based on the numerical integration using Rayleigh's-and-Sommerfeld's formulas without any approximations.

The value of the parameter α_o in each case was selected according to a predetermined maximum numerical aperture of the optical element NA_{max}:

$$\alpha_0 = \left[\frac{NA_{\max}}{\gamma(kR)^{\gamma-1}}\right]^{\frac{1}{\gamma}},\ \gamma \ge 1 \tag{33}$$

where R – is the radius of the optical element.

Numerical simulation was performed with the following designed parameters: $\lambda = 1$ μm , the maximum numerical aperture $NA_{max} = 0.95$, the radius $R = 10\,\lambda$.

Fig. 4 shows the results of diffraction of a flat limited beam on microelements at different values of γ.

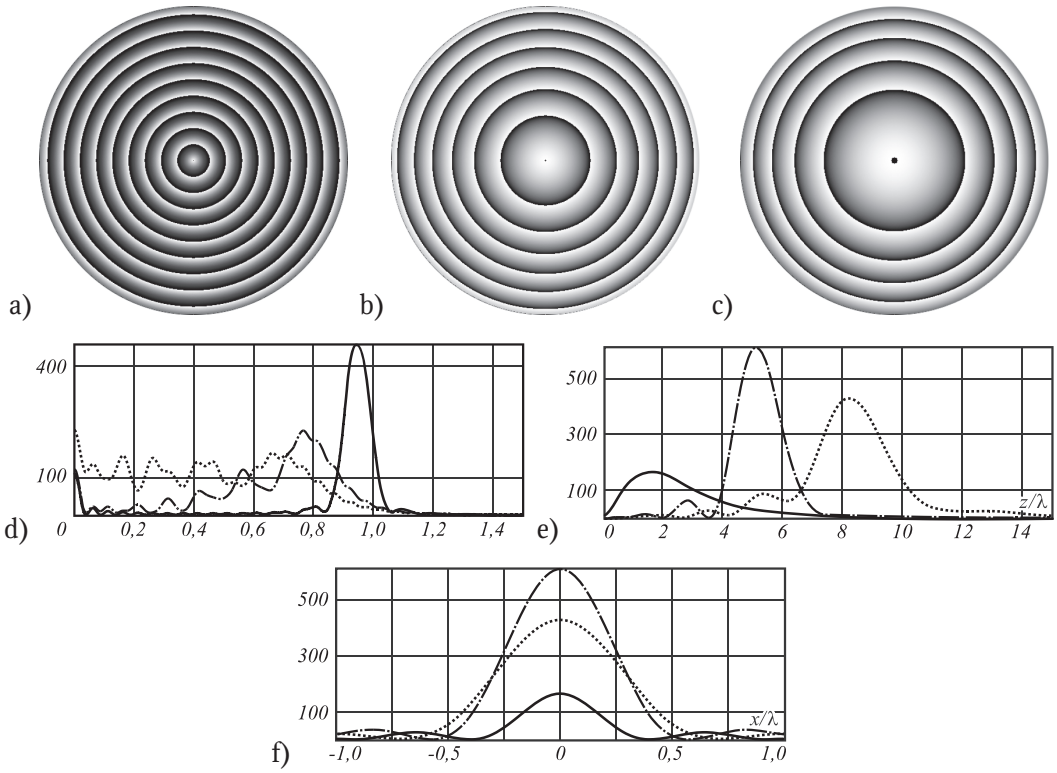

Fig. 4. Fracxicon phase at (a) γ = 1, α_0 = 0,95, (b) γ = 1,5, α_0 = 0,185, (c) γ = 2, α_0 = 0,087 and the relevant spatial spectral distributions (d); as well as distribution sof intensity along the optical axis (e) and in the plane of the maximum value (f) (γ = 1 – is a continuous line, γ = 1.5 – is a dash-and-dot line, γ = 2 – is a dotted line)

As seen from Fig. 4 a–c, the frequency of circular lines for the axicon is uniform, while it is condensed in periphery for the fracxicon $\gamma > 1$ and the lens. It is clearly seen from the spatial spectrals that the fracxicon occupies an intermediate position between the lens, whose spectrum is almost uniformly distributed in the frequency range from 0 to 0.8 and the axicon, the spectrum of which is concentrated about the frequency of 0.95.

The longitudinal propagation of intensity shows that in a nonparaxial mode it is possible that the fraxicon provides much better energy concentration than the lens (Fig. 4d). In this case the dimension of a focal spot turns out to be smaller in the plane of the maximum intensity than at the lens (Fig. 4e); the lens light-spot diameter equals, by a level of the intensity halftime, to 0.62λ – for the lens at the distance of z = 8.25λ, to 0.51λ – for the fracxicon at the distance of z = 5.14λ and to 0.38λ – for the axicon at the distance of z = 1.7λ.

For the parabolic lens in section 2 the right boundary of a light segment has been evaluated, which can be considered as a focal length $z_{\max} = 1/(2k\alpha_0^2)$. For considered parameters it turns out to be 10.5λ that is by 27% more than if obtained numerically.

For the fracxicon we can use the formula (11), from which the plane of the maximum intensity shall be forecasted at a distance of z_{max} = 5,54λ, that is by 8% more than if obtained numerically.

In paper [30] we considered the axicon in the nonparaxial case and obtained an expression for the boundary of the light segment, which had coincided with a well-known formula of the length of the light segment generated by the axicon [33] $z_{\max} = R\sqrt{1-\alpha_0^2}/\alpha_0$. Using this formula we can roughly determine the distance of the maximum intensity which, for the considered parameters, is z_{max} = 3,28λ, that is almost two times higher than if obtained numerically.

Such overestimated evaluations of theoretical values relate to the fact that they predict not the position of the maximum intensity, but the beginning of the shadow boundary which is located right-handed of the maximum.

Let us, however, note that the parabolic lens is not optimal for the beam focusing in the nonparaxial case. It is known that the best focusing can be provided by an aberration-free (hyperbolic) lens:

$$\tau_{lens}(r) = \exp\left(-ik\sqrt{r^2+f^2}\right) \qquad (34)$$

where f – is a focus distance.

Fig. 5 shows the results of focusing the plane beam limited with a radius R=10λ =with a microlens (34)

at different focus distances. The foci were chosen so as to correspond to distances of the maximum intensity of the above components – f =1.7λ. (Fig. 5a), f =5.14λ. (Fig. 5b), f =8.25λ (Fig. 5c). By comparing Fig. 4a–c and Fig. 5a–c we can see that the structure of the element phase concentrating the beam on defined planes is very similar, even up to and including the transformation of the hyperbolic lens (34) to the axicon at low values of the focus distance f.

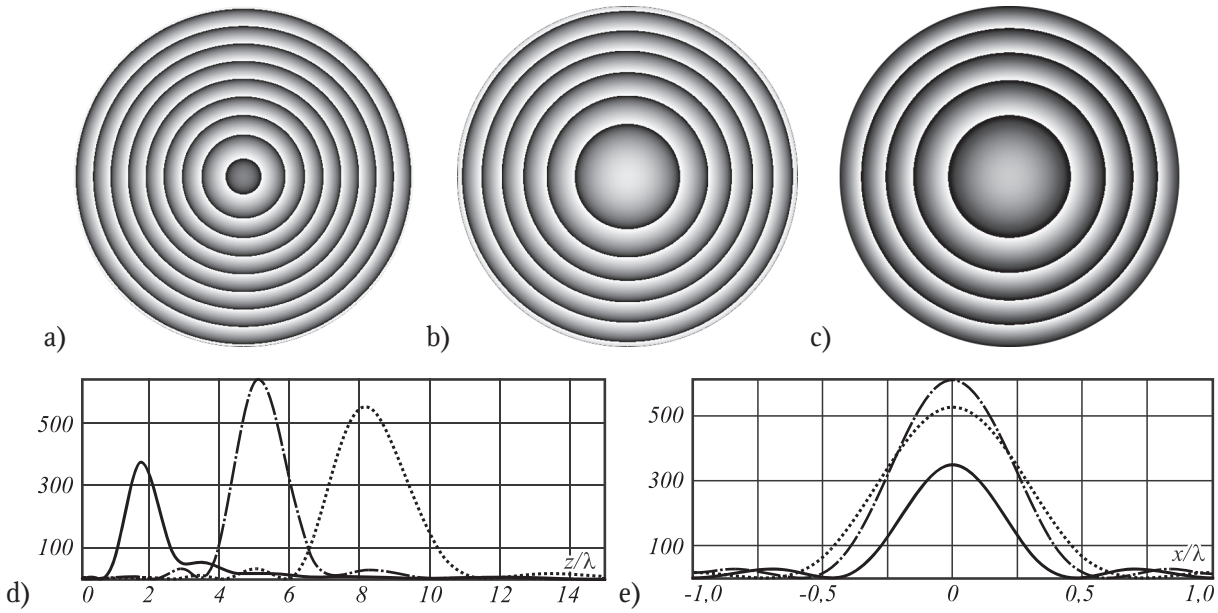

Fig. 5. Phase of the hyperbolic lens (34) at (a) f = 1.7λ, (b) f = 5.14λ, (c) f = 8.25λ and the relevant distributions of intensity (d) along the optical axis, and (e) in planes of focuses (f = 1.7λ. – is a continuous line, f = 5.14λ – is a dash-and-dot line, f = 8.25λ – is a dotted line)

The comparison of the longitudinal distribution of intensity (Fig. 4e and Fig. 5f) shows that the lens (34) provides better energy concentration than the above considered microcomponents. However, the situation with a dimension of the light spot is ambiguous. Diameter of the light spot of the hyperbolic lens with f = 1.7λ equals to 0.42λ that is by 10% greater than that of the axicon when the intensity is double increased. Results for the lens (34) and the fracxicon with γ = 1.5 are very close to each other both by the energy concentration, and also by the dimension of the light spot (for f = 5.14λ the light spot dimension equals to 0.514λ that is by 1% higher at the increase of intensity by 4%). For the focus f = 8.25λ the dimension of the light spot is the same as that one of the parabolic lens 0.62λ, when the intensity is increased by 20%.

Thus, we can conclude that in the nonparaxial area the fracxicon with an exponent within the mid-range of $1 < \gamma < 2$ is actually an analogue of the hyperbolic lens optimally focusing the incident beaming. Let us here by note that when using the fracxicon the sharper shade is provided at the right of the maximum, if compared to that one, when using the hyperbolic lens (Fig. 4e and 5d compared).

Conclusion

In this paper we have examined the effect of the fracxicon as a transition element between the parabolic lens and the axicon in the nonparaxial wave model.

Based on the modified method of the stationary phase, the approximate analytical expressions have been obtained for distribution of the complex amplitude on the optical axis in the diffraction of the plane wave on the fracxicon with an exponent of $1 < \gamma < 2$.

Numerical simulations have shown that at high numerical apertures the fracxicon with an exponent close to 3/2 is actually an analogue of the hyperbolic lens optimally focusing the incident beaming.

Acknowledgements

The work has been performed with the support of the Ministry of Education and Science of the Russian Federation and the Russian Foundation of Basic Research (RFBR) grant 13-07-97004-r_povolzhe_a.

References

1. McLeod, J.H. The axicon: a new type of optical element / J.H. McLeod // Journal of the Optical Society of America. – 1954. – Vol. 44. – P. 592-597.

2. Fujiwara, J. Optical properties of conic surfaces. I. Reflecting cone / J. Fujiwara // Journal of the Optical Society of America. – 1962. – Vol. 52. – P. 287-292.

3. Sochacki, J. Annular-aperture logarithmic axicon / J. Sochacki, Z. Jaroszewicz, L.R. Staronski and A. Kolodziejczyk // Journal of the Optical Society of America. – 1993. – Vol. 10. – P. 1765-1768.

4. Jaroszewicz, Z. Apodized annular-aperture logarithmic axicon: smoothness and uniformity of the intensity distribution / Z. Jaroszewicz, J. Sochacki, A. Kolodziejczyk and L.R. Staronski // Optics Letters. – 1993. – Vol. 18. – P. 1893-1895.

5. Golub, I. Characterization of a refractive logarithmic axicon / I. Golub, B. Chebbi, D. Shaw, and D. Nowacki // Optics Letters. – 2010. – Vol. 35. – P. 2828-2830.

6. Sochacki, J. Nonparaxial design of generalized axicons / J. Sochacki, A. Kolodziejczyk, Z. Jaroszewicz and S. Bara // Applied Optics. – 1992. – Vol. 31. – P. 5326-5330.

7. Davidson, N. Holographic axilens: high resolution and long focal depth / N. Davidson, A. Friesem and E. Hasman // Optics Letters. – 1991. – Vol. 16(7). – P. 523-525.

8. Koronkevich, V.P. Lensacon / V.P. Koronkevich, I.A. Mikhaltsova, E.G. Churin and Yu.I. Yurlov // Applied Optics. – 1993. – Vol. 34(25). – P. 5761-5772.

9. Parigger, C. Spherical aberration effects in lens axicon doublets: theoretical study / C. Parigger, Y. Tang, D.H. Plemmons [et al.] // Applied Optics. – 1997. – Vol. 36(31). – P. 8214-8221.

10. Khonina, S.N. The lensacon: nonparaxial effects / S.N. Khonina, N.L. Kazanskii, A.V. Ustinov, S.G. Volotovskiy // Journal of Optical Technology. – 2011. – Vol. 78 (11). – P. 724-729.

11. Bin, Z. Diffraction property of an axicon in oblique illumination / Z. Bin and L. Zhu // Applied Optics. – 1998. – Vol. 37. – P. 2563–2568.

12. Burvall, A. Axicon imaging by scalar diffraction theory / A. Burvall. – PhD thesis. – Stockholm. – 2004.

13. Khonina, S.N. Axicons application in imaging systems for increasing depth of focus / S.N. Khonina, D.A. Savelyev // Bulletin of Samara Scientific Center of RAS. – 2011. – Vol. 13(6). – P. 7-15. (In Russian).

14. Van Heel, A.C.S. Modern alignment devices // Advanced Optical Techniques; Ed. By A.C.S. Van Heel. – North-Hollandю – 1967. – P. 319.

15. Wang, K. Influence of the incident wave-front on intensity distribution of the nondiffracting beam used in large-scale measurement / K. Wang, L. Zeng, and Ch. Yin // Optics Communications. – 2003. – Vol. 216. – P. 99-103.

16. Fortin, M. Optical tests with Bessel beam interferometry / M. Fortin, M. Piche and E.F. Borra // Optics Express. – 2004. – Vol. 2(24). – P. 5887-5895.

17. Reichelt, S. Self-calibration of wavefront testing interferometers by use of diffractive elements / S. Reichelt, H. Tiziani and H. Zappe // Proceeding of SPIE. – 2006. – Vol. 6292. – P. 629205-10.

18. Arimoto, R. Imaging properties of axicon in a scanning optical system / R. Arimoto, C. Saloma, T. Tanaka and S. Kawata // Applied Optics. – 1992. – Vol. 31(31). – P. 6653-6657.

19. Lu, J. Diffraction-limited beams and their applications for ultrasonic imaging and tissue characterization / J. Lu and J.F. Greenleaf // Proceeding of SPIE. – 1992. – Vol. 1733. – P. 92-119.

20. Ding, Z. High-resolution optical coherence tomography over a large depth range with an axicon lens / Z. Ding, H. Ren, Y. Zhao, J.S. Nelson and Z. Chen // Optics Letters. – 2002. – Vol. 27. – P. 243-245.

21. Leitgeb, R.A. Extended focus depth for Fourier domain optical coherence microscopy / R.A. Leitgeb, M. Villiger, A.H. Bachmann, L. Steinmann and T. Lasser // Optics Letters. – 2006. – Vol. 31(16). – P. 2450-2452.

22. Lee, K.-S. Bessel beam spectral-domain high-resolution optical coherence tomography with micro-optic axicon providing extended focusing range / K.-S. Lee and J.P. Rolland // Optics Letters. – 2008. – Vol. 33(15). – P. 1696-1698.

23. Arlt, J. Optical micromanipulation using a Bessel light beams / J. Arlt [et al.] // Optics Communications. – 2001. – Vol. 197. – P. 239-245.

24. Garces-Chavez, V. Simultaneous micromanipulation in multiple planes using a self reconstructing light beam / V. Garces-Chavez [et al.] // Nature. – 2002. – Vol. 419. – P. 145-147.

25. Khonina, S.N. DOE for optical micromanipulation / S.N. Khonina, R.V. Skidanov, A.A. Almazov, V.V. Kotlyar, V.A. Soifer, A.V. Volkov // Proceedings of SPIE: Lasers and Measurements. – 2004. – Vol. 5447. – P. 304-311.

26. Shao, B. Size tunable three-dimensional annular laser trap based on axicons / B. Shao, S.C. Esener, J.M. Na scimento, M.W. Berns, E.L. Botvinick and M. Ozkan // Optics Letters. – 2006. – Vol. 31. – P. 3375-3377.

27. Khonina, S.N. Fractional axicon as a new type of diffractive optical element with conical focal region / S.N. Khonina, A.V. Ustinov, S.G. Volotovsky // Precision Instrument and Mechanology. – 2013. – Vol. 2(4). – P. 132-143.

28. Ustinov, A.V. Geometrooptic analysis of generalized refractive lenses / A.V. Ustinov, S.N. Khonina // Bulletin of Samara Scientific Center of RAS. – 2012. – Vol. 14(4). – P. 28-37. (In Russian).

29. Ustinov, A.V. Generalized lens: calculation of distribution on the optical axis / A.V. Ustinov, S.N. Khonina // Computer Optics. – 2013. – Vol. 37(3). – P. 307-315. (In Russian).

30. Ustinov, A.V. Analysis of flat beam diffraction by divergent fracxicon in nonparaxial mode / A.V. Ustinov, S.N. Khonina // Computer Optics. – 2014. – Vol. 38(1). – P. 42-50. (In Russian).

31. Ditkin, V.A. Integral transforms and operational calculus / V.A. Ditkin and A.P. Prudnikov. – Moscow: "Fizmatlit" Publisher. – 1961. – Charters VII, VIII. (In Russian).

32. Ustinov, A.V. Analysis of laser beam diffraction by axicon with the numerical aperture above limiting / A.V. Ustinov, S.N.

Khonina // Computer Optics. – 2014. – Vol. 38(2). – P. 213-222. (In Russian).

33. Durnin, J. Diffraction-free beams / J. Durnin, J.J. Miceli and J.H. Eberly // Physics Review Letters. – 1987. – Vol. 58(15). – P. 1499-1501.